Theses and Dissertations   Graduate School

2020

Comparing coastal storm impact to decadal change in barrier island ecosystems

Philip A. Tuley

Comparing coastal storm impact to decadal change in barrier island ecosystems

A thesis submitted in partial fulfillment of the requirements for the degree of
Master of Science at Virginia Commonwealth University

by

Philip A. Tuley
Master of Science, Virginia Commonwealth University, 2020
Bachelor of Science, Virginia Commonwealth University, 2018
Associate of Science, John Tyler Community College, 2016

Major Director: Dr. Julie C. Zinnert
Assistant Professor, Department of Biology

Virginia Commonwealth University
Richmond, Virginia
May, 2020

Table of Contents

List of Figures

List of Tables

Abstract

COMPARING COASTAL STORM IMPACT TO DECADAL CHANGE IN BARRIER ISLAND ECOSYSTEMS

By Philip A. Tuley

A thesis submitted in partial fulfillment of the requirements for the degree of

Virginia Commonwealth University, 2020

Major Director: Dr. Julie C. Zinnert, Assistant Professor, Department of Biology

Highly dynamic coastal systems respond to disturbance events with a combination of topographic and vegetative changes. With rising sea level, barrier islands migrate toward main land via a movement of upland cover onto backbarrier marsh. While the impacts of sea level rise on barrier islands is understood, studies of vegetation responses to coastal storms on barrier islands are limited. Here we quantified barrier island vegetation change in response to an isolated storm event and compared to long-term (multi-year) periods. We hypothesized that disturbance-resisting areas with high woody vegetation cover and/or high foredune elevation would experience minimal transitions after a storm event, whereas disturbance-reinforcing areas with low vegetation cover and low foredune elevation would experience greater transitions between ecosystem states after a storm event. Storm occurrences were identified utilizing meteorological station from a regionally-central barrier island. 575 storms were identified and the storm of greatest intensity was further analyzed. Remote sensing vegetation classifications of pre- and post-event imagery were used to measure vegetative change and compared to longer temporal change. Patterns of dissonance were found at the island-scale, as net loss of woodland cover occurred during the storm and a net increase was observed through decadal regimes. This is indicative of a slow growing late successive vegetation responding to disturbance. Using 1 km

cross islands transects, significant correlations between stable upland vegetation covers (both woodland and grassland) and percent bare suggests that the amount of upland land cover may be important in upland community response to storm events. Maximum bare elevation was significantly correlated to woodland cover, indicative of disturbance resisting domains. Significant correlations found between pre-storm woodland cover (both area and percent) and non-changing grasslands suggest that the existence of woody vegetation is dependent on the establishment and extent of stable grasslands. No correlations were found with area of marshland converted to upland post storm. My results did not support my hypothesis but rather display upland vegetation interaction amidst a moderate coastal storm.

Introduction

Barrier island systems are the first line of protection (Feagin et al., 2015; Otvos, 2012; Spalding et al., 2014; Temmerman et al., 2013) for 10% of coastlines worldwide (Stutz & Pilkey, 2011). Topography and vegetative cover determines the response to long-term and short-term disturbance events (Feagin et al., 2015; McBride et al., 1995; Zinnert et al., 2017; Zinnert et al., 2019; Figure 1). Storms are stochastic and create disturbances through sediment movement (erosion, accretion, overwash), saltwater flooding, wind gusts, and extreme shear wind force (Hayden et al., 1995; Sallenger Jr., 2000). Storm disturbance may lead to changes in the morphology of the island, vegetation, or complete loss of habitat (Gornish & Miller, 2010; Miller et al., 2010; Zinnert et al., 2019). Barrier islands respond to sea-level rise by migrating landward; however, coastal storms increase the instantaneous sea-level beyond what is predicted (i.e. storm surge) and may increase rates of migration (i.e. sediment deposition via overwash of upland island sediments onto the backbarrier marsh; Leatherman, 1982; Leatherman, 1983).

Along the Atlantic coast, storm events consist of tropical cyclones (i.e. hurricanes) and extratropical cyclones (i.e. nor'easters), both of which can drive an isolated rise in sea level and winds greater than 33 m s^{-1} (Dolan & Davis, 1993). Nor'easter waves may range from 1.5 – 10 m high, often occurring over several days and strongly influence coastal morphodynamics (Dolan & Davis, 1993), whereas hurricane storm surge does not last as long. Storm location and wind strength are not good predictors for quantifying localized nor'easter disturbance, as a nor'easter 1500 km from the coast may still produce waves damaging to the coastline; conversely, hurricanes typically leave a narrow 100-150 km path of disturbance (Dolan & Davis, 1993). Intensity of extreme storm events are predicted to increase in the face of anthropogenic climate change (Knutson et al., 2010; Grinsted et al., 2013). Regardless of storm type, dune elevation

and vegetative cover are important consideration for quantifying storm impact to coastlines (Sallenger Jr., 2000; Zinnert et al., 2017).

Established foredunes offer resistance to storm disturbance and minimize overwash frequency (Doing, 1985; Zinnert et al., 2019). Vegetative communities influence sediment capture and transport rates. Plant stems and roots impede aeolian (wind) transport, accrete sediment, and enhance sediment stabilization (Feagin et al., 2015; Silva et al., 2016). Various growth forms (i.e. grass, forbs, woody, etc.) influence the efficiency of sediment capture (Gilbert & Ripley, 2010) and woody vegetation is known to stabilize areas during storm events (US Army Corps of Engineers, 2013). Barrier islands in the mid-Atlantic express two stability domains based on topography-vegetation interactions: disturbance-resisting and disturbance-reinforcing (Zinnert et al., 2017; Zinnert et al., 2019). Disturbance-resisting coastlines are typically composed of dune-swale complex, exhibit structural vegetative diversity, and impede overwash of sediments, often resulting in erosion with disturbance events (Figure 2A, B). Disturbance-reinforcing coasts have low topography, consist of burial-tolerant vegetation with little to no woody cover, and are frequently overwashed during storm events as there is little resistance to sediment movement (Figure 2, D). It is suggested that repetitive overwash events may increase primary dune susceptibility to future storm disturbance (Long et al., 2014). This study fills a knowledge gap on how an isolated storm impacts barrier islands in the context of disturbance-resisting and disturbance-reinforcing stability domains.

Over recent decades, remote sensing has allowed us to better observe and quantify processes at the landscape-scale, which is highly relevant in coastal areas that experience frequent storm events. Remote sensing is the leading method in observing coastal disturbances such as hurricanes and relative sea level rise (RSLR), (Bazzichetto et al., 2016; Bukata et al.,

2018; Danilo & Melgani, 2019; Macleod & Congalton, 1998; Ozesmi & Bauer, 2002; Shalaby &

Tateishi, 2007; Valderrama-Landeros & Flores-de-Santiago, 2019; Zinnert et al., 2019). Using

remote sensing, temporal changes on the landscape can be monitored over decades (Hermosilla

et al., 2019; Lee & Park, 2019; Zinnert et al., 2016) or pre/post disturbance event (e.g., fire,

flooding, deforestation; Christopoulou et al., 2019; Sánchez-Azofeifa et al., 2001). Landscape

assessment pre and post coastal storm allows for rapid quantification of change due to

disturbance, which may otherwise be limited due to access and recovery efforts (Aosier &

Kaneko, 2007; Ayala-Silva & Twumasi, 2004; Lee et al., 2008; Ramsey III et al., 1997; Ramsey

III et al., 1998; Ramsey III et al., 2001; Wang et al., 2010). Here, we fill a knowledge gap by

assessing pre and post storm event landscape change on a barrier island in the context of stability

domains, which may provide a framework for predicting storm related disturbance response.

  Using remotely sensed data, my objective is to assess transitions between ecosystem

states (i.e. grassland, woodland, ocean, marshland, and exposed sand) before and after a storm

event. I hypothesize that 1) disturbance-resisting areas with high woody vegetation cover and/or

high foredune elevation will have minimal transitions after a storm event (**A ➜ B** Figure 2),

whereas 2) disturbance-reinforcing areas with low vegetation cover and low foredune elevation

will experience higher rates or transitions between ecosystem states after a storm event (**C ➜ D**

Figure 2).

Methods

  The Virginia Coast Reserve (VCR) (Figure 3), a Long-Term Ecological Research

(LTER) site, is a hotspot of RSLR in the U.S. (~5.2 mm yr^{-1}; Piecuch et al., 2018). This system is

>14,000ha, consists of a net northern longshore current, and has an average ~ 7m yr^{-1} of

coastline retreat that varies by location (Deaton et al., 2017; Zinnert et al., 2019). The VCR consists of a system of 13-barrier islands, lagoons, and an extreme rate of land cover change (i.e. barrier island transgression due to RSLR and coastal storms; Hayden et al., 1991). This study focuses on ~80 km of 9 undeveloped barrier islands. Islands of focus are solely on the Atlantic coast of Virginia and are separated from the mainland by a lagoon system. This site is undergoing a well-documented landscape-wide ecosystem homogenization as the changing climate has induced expansion of a native-invasive shrub beyond its historic range (Knapp et al., 2008; McCaffrey & Dueser, 1990; Young et al., 1994; Young et al., 1995a; Zinnert et al., 2019).

Storm analysis

In order to identify the storm event used in this study, we quantified storm events between 2013 – 2018. We followed the methods of Dolan and Davis (1992) to quantify isolated storm events. The Dolan-Davis Power Index (DDPI) (*equation 1*), where P is power, H is maximum wave height, and t_D is hours of storm duration.

Equation 1
$$P = (H)^2 t_D$$

Archives of atmospheric and oceanic records were obtained from the Wachapreague buoy of the National Buoy Center and from the VCR Hog Island meteorological station. Records were pre-processed so that all records represent the same time interval (1-hour) and incomplete records were removed. For the purpose of this study *storm duration* will follow the American Meteorological Society (2012) definition of rainfall occurrence. We define system-wide rainfall as precipitation >0.05mm with an allowance of records >0.02mm which proceed or succeed a

record of >0.05mm. As this study incorporated the entire island chain, neither the effect of a

single pressure cell (nor the interactions between cells) can be fully represented from merely 1,

2, or 3 remote meteorological stations. To accommodate for this, we incorporated all

precipitation-breaks up to 12 hours within the definition of a single storm. We selected the most

intense storm event within the time period observed for further analysis.

Imagery analysis

Satellite imagery was used to analyze the spatial effects of a coastal storm to the island

chain. Storm imagery was collected July 25, 2015 (Landsat 8) and October 21, 2015 (Landsat 8),

before and after the selected storm. Landsat 8 Operational Land Imager (OLI) consists of 9-

spectrial bands at 15 m^2 and 30 m^2 resolutions; only the 30 m^2 resolution was used for this study.

Landsat Imagery was used to classify land cover into the following vegetation classes: woodland,

grassland, marshland, exposed sand (bare), and ocean following the methods of a supervised

classification from Zinnert et al. (2011, 2016, 2019). For the storm of interest, imagery was

collected directly before and directly after the event to identify immediate storm forced

ecosystem changes. A comparison was performed between imagery to quantify areas of land

cover change and stability post storm disturbance. Each image file was radiometrically corrected

using ENVI 4.7 and predefined ENVI settings for Landsat calibration using ENVI QUAC. The

focal storm land cover change was then compared to a set of decadal imagery; each decadal

period consists of a multitude of storm events (Figure 4). Decadal imagery was obtained from

Zinnert et al. (2019) from September 21, 1984 (Landsat TM5), September 12, 1998 (Landsat

TM5), August 12, 2011 (Landsat TM5), and September 12, 2016 (Landsat 7). The imagery from

1984, 1998, 2011, and 2016 was previously classified and analyzed (Zinnert et al., 2019), the

remaining methods are specific to the July 2015 and October 2015 imagery surrounding the focal storm.

Regions of interest (ROI) were selected for each land cover type within each scene based on geo-rectified aerial photography. After ROIs were selected, supervised classifications using Landsat bands 1, 2, 3, 4, 5, and 7 were performed using maximum likelihood methodology. Classified scenes were converted to shapefiles within ENVI and exported to ArcGIS 10.4.1 (ESRI, 2016).

Analysis of land cover change

Pre-post storm area change was assessed at both the island and the island chain scale to represent landscape change. Changes in land cover classes between scenes were quantified by overlaying the class of interest from the pre-storm scene with the class of interest from the post-storm scene. Overlapping layers were intersected and areas were summed for a pairwise comparison of each land cover class. Previous remote sensing studies of this island chain used 1km sub-samples perpendicular to each island's oceanic coastline (Nettleton, 2018; Zinnert et al., 2019); this study used a similar but higher resolution (500m) sub-sampling technique, which excluded northern and southern tips of islands where coastal-processes are more dynamic (Stallins & Corenblit, 2018). Sub-samples were created for each island in ArcGIS with the fishnet tool. The resulting shapefile was rotated with the editor tool until the rows were perpendicular to the coast of the island (Figure 5). The area of vegetation change/stability by sub-sample was collected by intersecting the pre-storm imagery with the post-storm imagery and the sub-sample file. We defined land cover stability as vegetation (pre-storm) which did not shift to a different vegetative land cover post-storm. Elevation was derived from a LiDAR Digital Elevation Model (DEM) available from CoNED. The DEM was used to mask the pre- and post-

storm imagery and erase classified terrain below mean sea level, to account for potential tide effects. Foredune elevation is a potential metric for protection from overwash and movement of sediment. For each sub-sample, maximum bare elevation on the shoreface was used to estimate foredune crest elevation. To perform this, the DEM was masked by the pre-storm bare vegetation class, and the Zonal Statistics tool was used to extract descriptive statistics for each zone, transect. Calculations of marshland to upland and upland to marshland were made by masking the upland-marshland boundary and using the intersect tool on aforementioned mask, pre-storm imagery, and the post-storm imagery. This was an attempt to reduce noise, such as sand deposits on the border of the marshland. Due to the patchy distribution of the upland-marshland boundary on Parramore Island, this island was removed from upland-marshland analysis.

Statistical Analysis

Elevation and intersected vegetation (area of pre-vegetationX and post vegetationX) data were transformed using natural log to meet normality assumptions. Pearson correlations were used on the sub-sample dataset to test for correlations among elevation, vegetation change, and stability across the system.

Results

575 storms were identified between 2013 – 2018 (Figure 6). The Dolan-Davis storm class determined 567 of these storms were *weak*, 7 were *moderate*, and 1 was *significant*. The singular *significant* storm occurred between September 29th and October 3rd 2015 and was associated with Hurricane Joaquin. Precipitation from this event reached 51.6 mm at the VCR with an average windspeed of 3.3 m s^{-1}, nearly double the average storm windspeed during in 2015. The focal storm had a duration of 79 hr and a max wave height of 1.74 m above mean sea level. The system experienced two hurricanes during the timeframe of storms analyzed in this study; Hurricane Gert (August 12-17, 2017) came within 595 km of the Virginia coast and Hurricane Michael (October 7-11, 2018) was demoted to a tropical storm while over the VCR. Both hurricanes were class 1 when closest to the Virginia barrier islands. These low-pressure systems registered as 14.8 and 37.1 DDPI, respectfully.

Landscape Storm Effects

Across all islands in this study, pre-storm net upland (woodland, grassland, and bare) was 3059 ha and experienced a 13.9% loss post-storm (424 ha). Comparatively, regional upland across decadal periods experienced 57.6% change in 1984-1998 (3328 ha), 57.6% change in 1998-2011 (1907.1 ha), and 30.4% change 2011-2016 (1145 ha). During a 79 hr period, these focal barrier islands lost 13.9% of upland land cover while this same region lost 30.4-57.6% across decadal periods. Despite the focal storm event having the lowest area change, when comparing decadal change expressed on a yearly basis, the 79 hour event had the highest rate of change of all periods, 424 ha storm^{-1}. During 2011-2016, the rate of change increased relative to previous timeframes and the focal storm may be a great contributor to this. Based on the rate of

change during the storm, upland land cover reorganization likely occurred following the focal storm.

A decadal shift of net upland loss to gain occurred since 1984 (Figure 8), from -1674 ha (1984-1998) to 422 ha (2011-2016). Bare ground experienced net lost from the system until 2011-2016 – but the amount gained during the storm (72 ha) may be significant when compared to that gained over the last 5 years. From 1984-1998 and 1998-2011, regional grassland net loss of -289.2 ha and -287.0 ha, respectfully during a time when there was net woody gain (Figure 8). In 2011-2016 grassland experienced a small landscape level net gain. Woody vegetation was mostly lost from the system in the storm event, whereas over decades woody cover increased. Pre-storm woody vegetation was moderately correlated to stable grass and pre-storm grass (area) ($r = 0.56$, $p = 0.0006$, $r = 0.60$, $p = 0.0003$, respectively, Table 1). Over time grass stability (i.e. area that has not changed between images) steadily decreased and woody stability steadily increased.

From calculating net land cover conversion at the island and sub-island scale, we compared patterns of land cover response from a storm event to decadal changes. During the 2015 storm period (Figure 9), a net gain of bare was observed on every island but Hog. Compared to the time series, bare land cover displayed a regional switch from complete net loss between 1984-1998 across all islands (ranging from 20.1 – 365.3 ha) to nearly a complete net gain between 2011-2016 in all but one island. Metompkin Island consistently experienced net loss of bare cover during this study. Between 1998-2011 (Figure 9), bare land cover conversion was variable across islands with losses and gains in no obvious pattern. Grasslands land cover was variable on each island during the focal storm. Islands with historic woody cover (Parramore, Hog, and Smith) experienced substantial grassland net gain during the storm (51.9

ha) amidst woody cover loss (86.9 ha). Parramore, and Smith Islands consistently experienced net loss of grassland cover within every decadal period, but during the storm event, grassland was gained.

The focal storm caused net loss of woodland cover on all islands where it was present (Figure 9). This differs from decadal changes where woody cover has been expanding (Figure 8). Gain of woodland cover from 1984-1998 occurred on three islands, Hog, Cobb, and Smith Islands. From 1998-2011, landscape gains were minimal as Cobb switched to a net loss of woodland cover. Woodland net change from 2011-2016 was variable from across all islands; Cobb and Hog Islands displayed a loss in woodland cover (31.1 ha and 4.2 ha, respectfully) – while the rest of the islands displayed net gain. Loss of woodland on most islands during the storm event does not explain landscape level gains during 2011-2016.

Sub-island Transects

We quantified land cover change across 131 transects on the 9 barrier islands. Conversion of backbarrier marsh to upland was used as an indicator of upland migration (i.e. transgression). Over 61 ha of marshland were converted to upland from the storm event (Figure 10). The greatest marsh to upland conversion rates occurred on Metompkin (6.3 ha), Cedar (3.9 ha), and Cobb (4.8 and 4.5 ha). There was high variation in marsh-upland conversions with no apparent patterns on islands or from north to south. There were no significant correlations between maximum bare elevation and both marsh to upland conversion or upland to marsh conversion ($r = -0.04$, $p = 0.8324$ and $r = -0.04$, $p = 0.8053$, respectfully) (Table 1). 18 transects had >1 ha of marsh to upland conversion with a highly variable maximum bare elevation range ($\mu = 3.26$ m and $\sigma = 1.37$ m). Although no significant correlations were found between marsh to upland and

the upland cover (stable area, pre-storm area, and pre-storm percent cover of bare, grassland, and woodland) there were trends with upland unvegetated cover (positive correlations) and upland vegetated cover (negative correlations). There was evidence of upland conversion to marsh on all islands (~31) (Figure 11). It is unknown if this is due to flooding along the marsh-upland boundary or permanent change. Maximum bare elevation values across islands was highly variable (Figure 12) and significantly correlated to woodland stability ($r = 0.41$, $p = 0.0170$) and pre-storm woodland cover, (woodland area, $r = 0.3$, $p = 0.0305$ and woodland % cover, $r = 0.36$, $p = 0.0425$) (Table 1). Maximum bare elevation values range from 7.93 m on Parramore to 1.85 m on Metompkin. The greatest maximum bare elevation change within an island occurred on Metompkin (5.29 m) and the smallest occurred on Myrtle (0.32 m).

Significant negative correlations were found between vegetated and unvegetated upland land cover (Table 1). Significant correlations were found in all upland vegetation interactions with percent cover of bare; while stable bare and pre-storm bare area were found significant with both percent of grassland and percent of woodland cover. This suggests that percent of the upland-classification may be important in upland community response to storm events. For example, percent unvegetated upland (bare cover) was negatively correlated with grassland stability and woodland stability ($r = -0.75$, $p < 0.0001$ and $r = -0.55$, $p = 0.0009$, respectfully) (Table 1). This suggests that upland area with greater vegetative cover has higher stability in a moderate coastal storm. Pre-storm woodland cover (both area and percent) was significantly correlated to grassland stability ($r = 0.57$, $p = 0.0006$ and $r = 0.41$, $p = 0.017$, respectfully) (Table 1). Pre-storm grassland area was found significantly correlated to pre-storm woodland cover (both area and percent) ($r = 0.60$, $p = 0.0003$ and $r = 0.47$, $p = 0.006$, respectfully) (Table 1).

These upland vegetation stability correlations suggest woodland cover is dependent on the establishment of successful grasslands (displayed as stable grasslands).

Discussion

The framework of stability domains has been applied to barrier islands at the dune level (Stallins, 2005; Vinent & Moore, 2014) and extended to the cross-island landscape (Zinnert et al., 2017; Zinnert et al., 2019) to explain the potential for overwash and disturbance related responses. Here, we assess pre- and post-storm event landscape change and relate it to decadal changes in the Virginia Coast Reserve barrier system. We evaluate this change in the context of stability domains by determining if relationships between maximum bare elevation and vegetation cover can predict land cover change (or the absence of change) after a single disturbance event, coastal storm. Although this has been found to explain transitions at decadal scales (Zinnert et al., 2019), we did not fully support the hypothesis that elevation and vegetation cover would predict transitions among ecosystem states. Specifically, the weak correlation between maximum bare elevation and the change or stability of vegetation during this storm was not sufficient at predicting marsh to upland conversion during a single storm event. Over decadal timescales, marshland to upland is influenced by elevation and woody vegetation (Zinnert et al., 2019). The significant positive correlation between pre woodland cover and woodland stability to elevation support the supported our hypothesis of lower transitions in disturbance-resistance domains.

Barrier islands are ideal locations to observe the effects of both long-term press and storm pulse perturbations on coastal vegetation. In this study, we document both system response to a single storm pulse and place in the context of long-term press and pulse events by comparing to decadal analysis. Despite the energy of nor'easters being spread across larger spatial area, there is reason for studying effects of extratropical coastal storms relative to hurricanes. Nor'easters occasionally experience stationary fronts, lengthening the duration of the localized presence of

the storm. In turn, this increases the opportunity for storm surge to compound with a high tide event, leading to coastal flooding. Nor'easters are also more common occurrences along the mid-Atlantic coast than hurricane events (Dolan & Davis, 1994). The focal storm occurred as a result of diabatic outflow from Hurricane Joaquin as a predecessor rain event (PRE) (Galarneau et al., 2010; Marciano & Lackmann, 2017). Based on Cote's (2007) classification, this storm does not meet the precipitation requirement (of 100mm day^{-1}) to be considered a PRE at the VCR; however, the focal storm did meet the qualifications nearby in South Carolina (Marciano & Lackmann, 2017). Despite the classification we give this storm, the focal storm registered a higher DDPI than two hurricanes that came close to the VCR during the 8-year timeframe of storm analysis.

The gradient in DDPI-class is indicative of localized disturbance along barrier island coasts. Coastal impacts the focal storm (240 on the DDPI) may have experienced, based on the *significant* storm (class 3), include overwash on low elevation profiles, and possible dune erosion without dune breaching (Dolan & Davis, 1992). These impacts demonstrate how stability domains (disturbance-reinforcing and disturbance-resisting) respond to disturbance due to the vegetative and geomorphic composition (Stallins, 2005; Vinent & Moore, 2014). Where foredune elevations are high (disturbance-resisting domain), disturbance events beyond the dune are less frequent than where foredune elevations are low (disturbance-reinforcing domain) (Figure 2) (Zinnert et al., 2017). In the occurrence of *severe* (class 4) or *extreme* storms (class 5), landscape-wide disturbance-resistant formations (i.e. high dune ridge) may be demolished due to breaching of dunes, overwash, and possibly mid-island inlet formation (Dolan & Davis, 1994). The focal storm reached a power of 240 on the DDPI, not close to the minimum power threshold for *severe* (929.03) or *extreme* (2322.58) DDPI classification. These hypotheses may apply to

storms of greater intensity than that observed here (registering as 240 on the DDPI). Mississippi-Alabama barrier islands (island-wide) response to tropical storm force winds from Hurricane Gustav depict rollover with stable/increased island area post-storm (disturbance-reinforcing) and erosion with reduced land area (disturbance- resisting) (Carter et al., 2018) (Figure 2). Vegetative regrowth is imminent and immediate; however, community species composition is variable (Carter et al., 2018; Snyder & Boss, 2002).

The focal storm event from this study still influenced significant land cover change when compared to decadal yearly rates of change. This is possibly due to storm imagery being captured immediately post storm, before the system could experience a recovery period. This is unlike the decadal imagery in which periods consist of long-term press (i.e sea-level rise) and pulse (i.e. storms) disturbance and recovery periods. Post-storm beach recovery can take upwards of 5 years, as seen after Hurricane Alicia (category 3, Saffir/Simpson Scale) (Morten et al., 1994). Within this recovery period, Morton et al., (1994) proposed a multistage idea of post storm recovery – forebeach accretion, backbeach accretion, dune restoration, and revegetation, all of which could occur within a decade.

Regional shoreline migration in Virginia increased from 5.1 m yr^{-1} (1850-1851) to 7.0 m yr^{-1} (2010), a rate >25x the average of mid-Atlantic and New-England shoreline migration (Deaton et al., 2017). Dissimilarities in shoreline change are present between historic (press) and isolated storm (pulse) regimes (Houser et al., 2018). Zinnert et al. (2019) show that all shoreline migration is not equal – some results from shoreface erosion (disturbance-resisting) and some results from island migration (quantified as marsh to upland conversion, disturbance-reinforcing). These land cover changes occur at the sub-island scale (Hsu & Stallins, 2019; Zinnert et al., 2019). We used this same approach and found sub-island change in both marsh to

upland and upland to marsh change caused by a single storm event. Maximum bare elevation was variable across the islands but weakly correlated to woodland cover. Although the context of stability domains for predicting island response was not apparent from this storm, this study shows that a single medium-level pulse event can cause change in the marsh-upland boundary.

Records show that woodland vegetation has expanded within this system (Young et al., 2007; Zinnert et al., 2019). Late-successive woodland establishment within this system consists primarily of the native-invasive shrub *Morella cerifera* (Collins & Quinn, 1982; Miller et al., 2010). Regional-scale decadal results of reduced grassland stability amidst woodland stability gains, support long-term trends of shrubland expansion into grassland patches (Figure 8). Shrubland encroachment onto grasslands is not merely a local trend (Knapp et al., 2008). Amidst coastal flooding, *M. cerifera* rapidly closes leaf stomata allowing it to survive overwash and storm surge associated with a *significant* storm (Young et al., 1995b). *Morella cerifera* produces a dense canopy, capable of shading out other species (Brantley & Young, 2007, 2009, 2010). The association of *M. cerifera* with *Frankia*, a nitrogen fixing bacterium, allows for successful establishment in a low nutrient environment (Wijnholds & Young, 2000; Young et al., 1992). Within the last 30 years, the local temperature has seldom exceeded the minimum temperature *M. cerifera* can survive and local microclimate modification is attributed to continued shrub encroachment (Huang et al., 2019). The changes observed between grassland and woody vegetation in this system are attributed to alternate stable states and may create novel scenarios for barrier islands during high sea-level rise (Huang et al., 2019, Zinnert et al., 2019).

Cobb Island is an example of a historic disturbance-resisting domain that switched to disturbance-reinforcing. It exhibited both coastline erosion, island rollover, and a large portion of the island exhibited change from this single storm (Figure 13). Extensive woody vegetation from

the 1990s resulted in shoreface erosion until woody vegetation was lost and rollover could take place (Zinnert et al., 2019). This erosion of Cobb is evident in the instability and dramatic net losses of woody vegetation occurring throughout the long-term temporal intervals. Now that woody vegetation has been essentially eroded from the island, Cobb Island had the greatest difference in transitions between marsh and upland (12.7 ha) and the highest marsh to upland transition (15.1 ha) in the system during a single storm event. This switch in domains could undergo an adaptive cycle, where initial recovery has potential of creating a novel ecosystem (Stallins & Corenblit, 2017).

Conclusion

This study builds on the framework of stability domains for understanding how isolated coastal storms may impact the Virginia barrier islands. Predicting coastal response to storms is difficult and historically focused on geomorphic features (i.e. beach width, dune height, etc., Houser, 2013; Morton et al., 1994; Sallenger Jr., 2000). This research moves beyond traditional metrics by incorporating interactions between topography and ecological processes, which have recently been demonstrated as an innovative framework for assessing broad scale land cover change in coastal systems (Zinnert et al., 2019). The Virginia barrier islands are impacted by both hurricanes and nor'easters and experience variable changes in sediment dynamics and vegetation cover (Deaton et al., 2017; Dolan & Davis, 1994; Young et al., 1995b; Zinnert et al., 2019). My findings suggest that a *moderate* storm event alters the landscape and contributes to decadal scale changes; however, this storm was not sufficient to observe changes associated with stability domains at the landscape scale. This study sets the groundwork for additional research of *severe* and *extreme* classed storms in the mid-Atlantic.
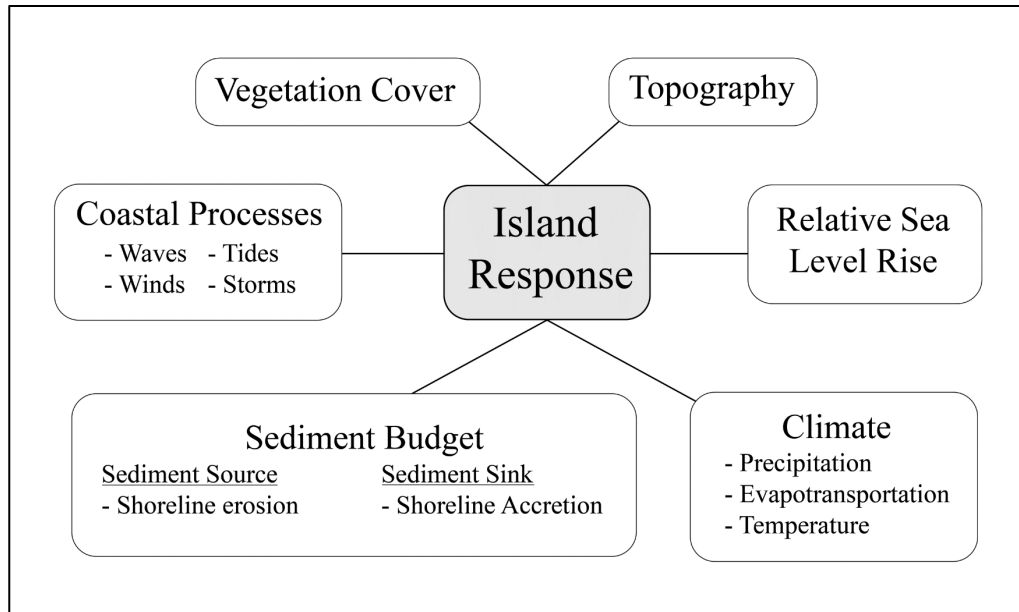
Figures

Figure 1: Representation of major barrier island modifiers. Figure modified from Thornton et al. (2000).
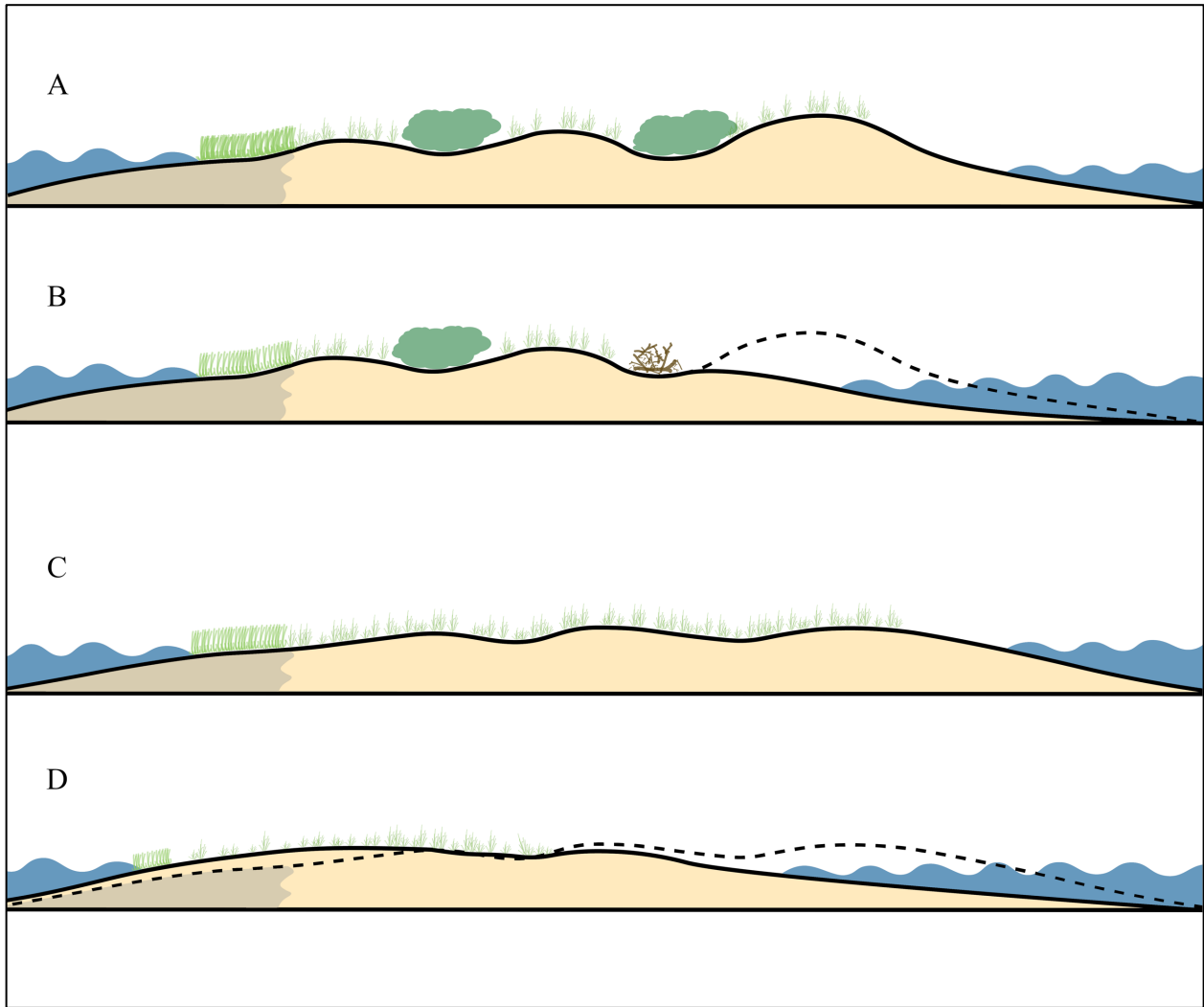
Figure 2: Cross-sections of high-relief disturbance-resisting island (A and B) and low-relief disturbance-reinforcing island (C and D). Note B and D erosion disturbance of A and C respectively. Figure modified from Zinnert et al. (2019).
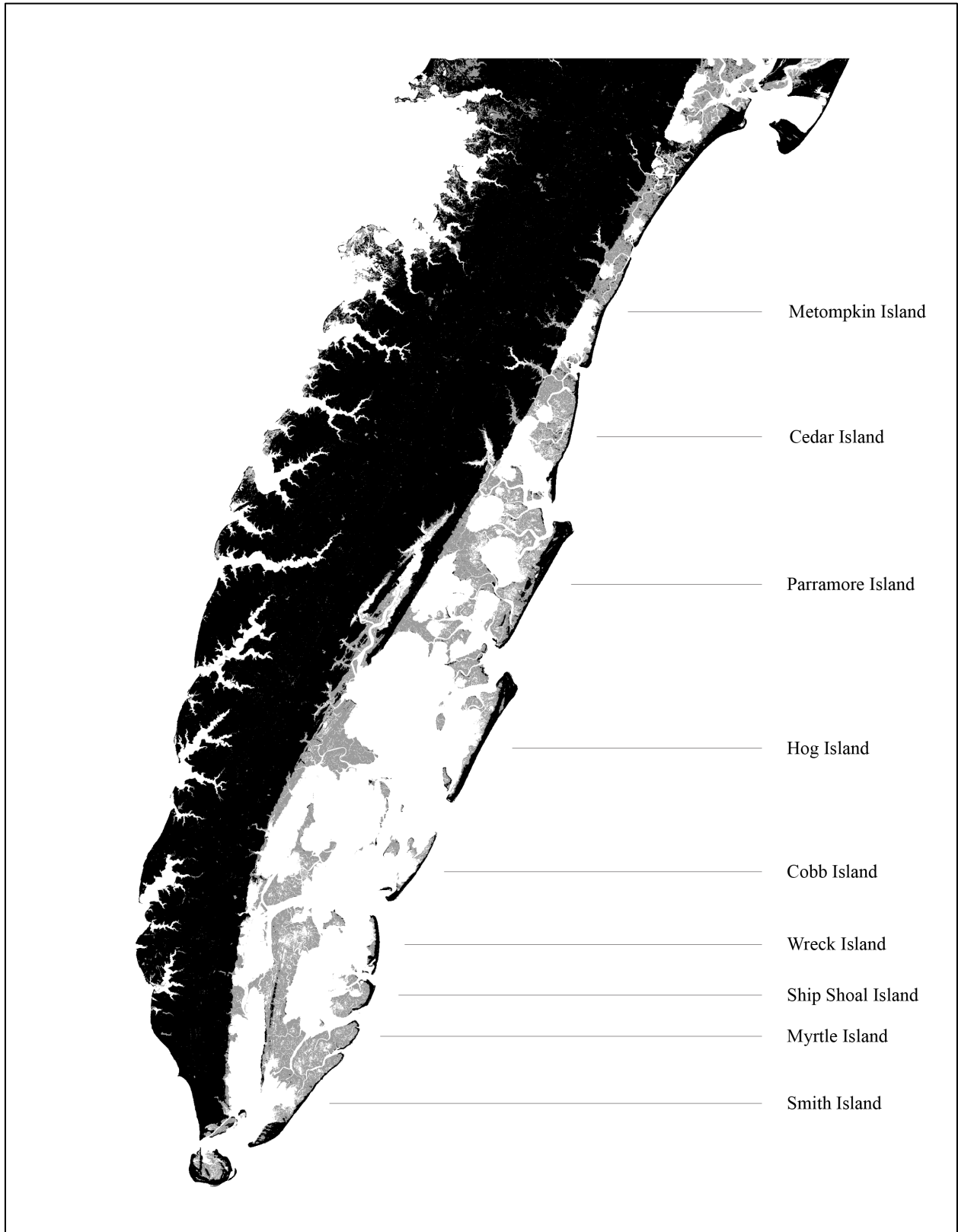
Figure 3: Map of the Virginia Eastern Shore and focal barrier islands for this study. Upland (terrestrial) area is represented in black and marsh is represented in grey. Data are classified from Landsat 8 Imagery on July 25, 2015.
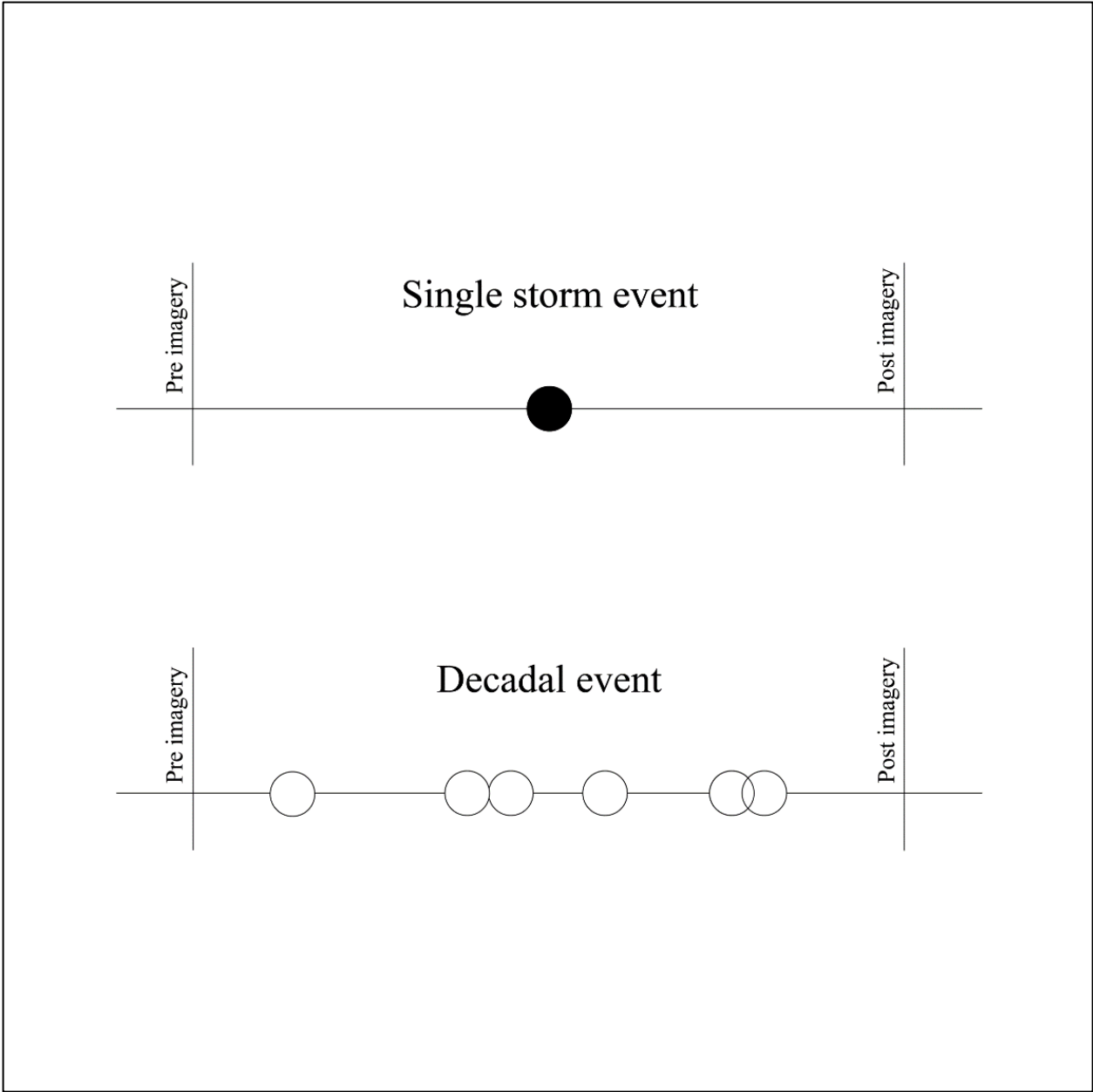
Figure 4: Display of the isolation of a single storm event period compared to multiple storms found in decadal event periods.

.
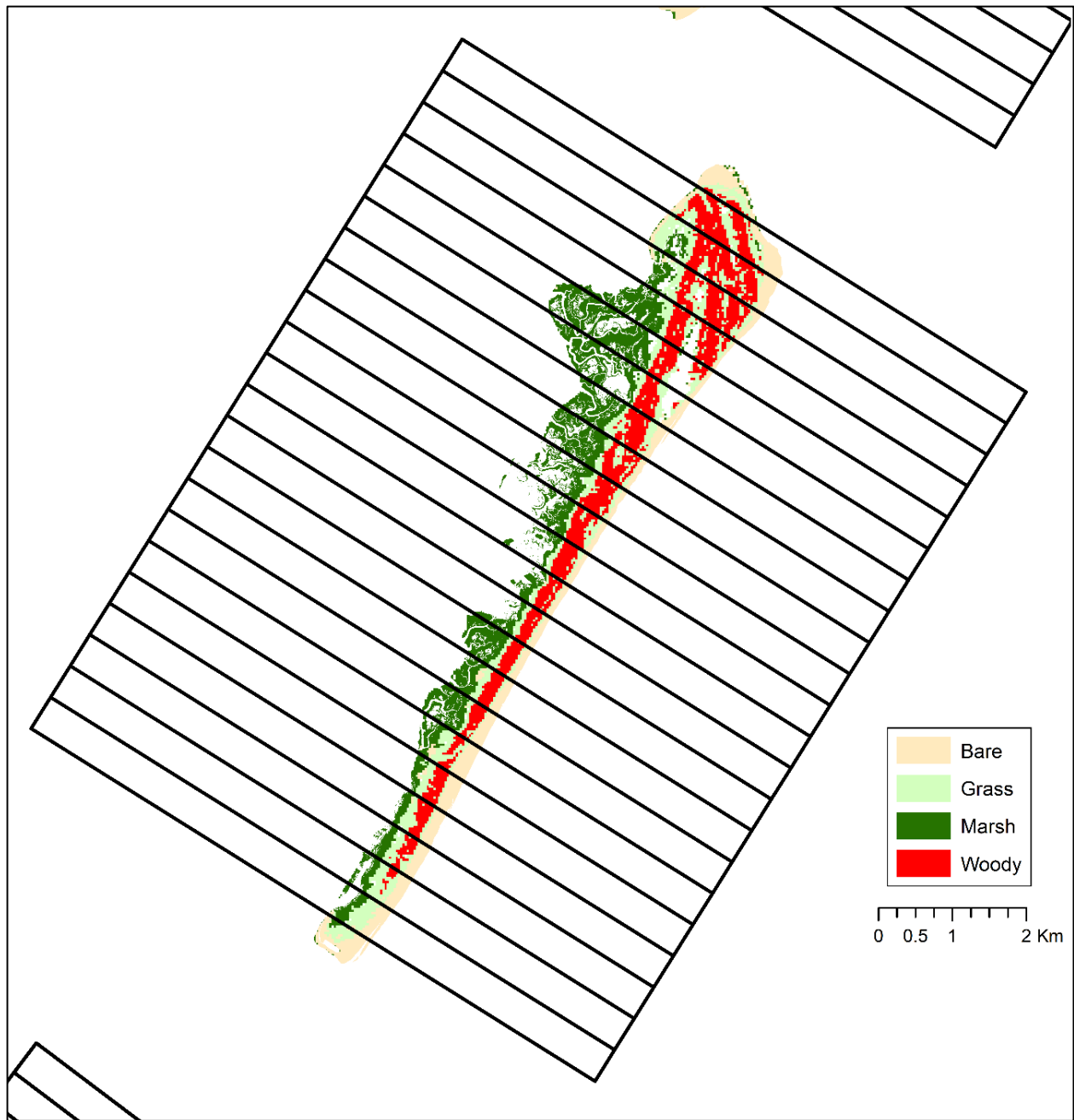
Figure 5: Map of Hog Island, Virginia displaying the sub-samples perpendicular to the coastline.
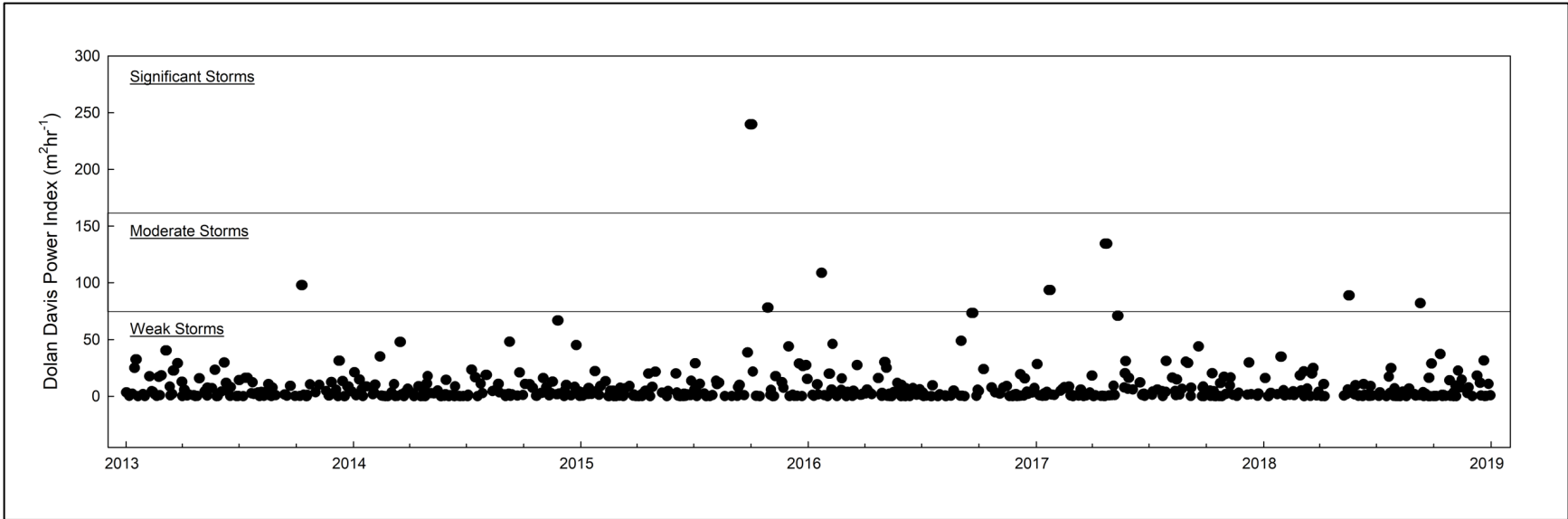
Figure 6: Storms identified – showing the Dolan Davis Power Index (DDPI) of each storm throughout 2013 – 2018.

.
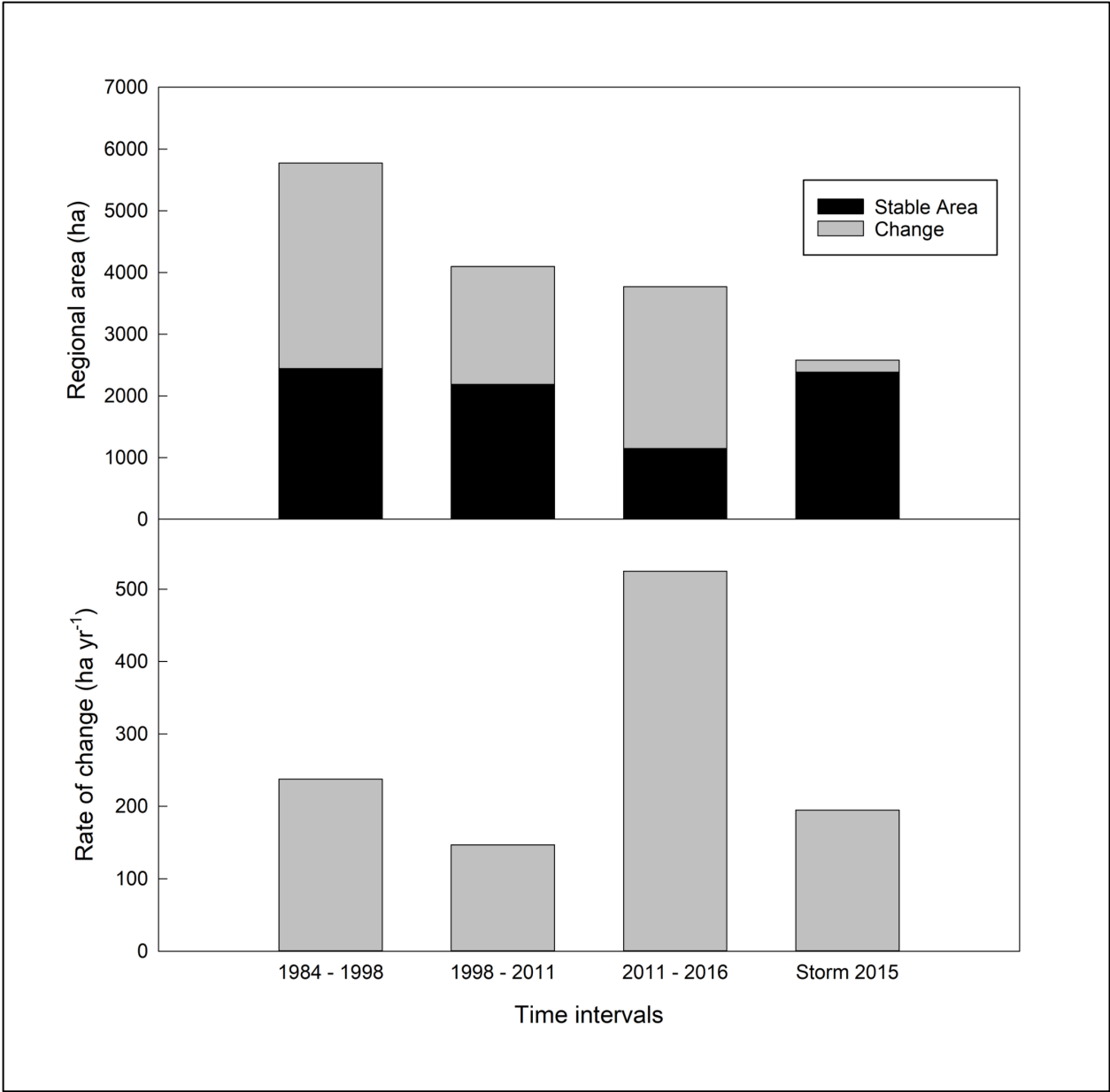
Figure 7: Regional total upland land cover area and rate of change within each period.

.
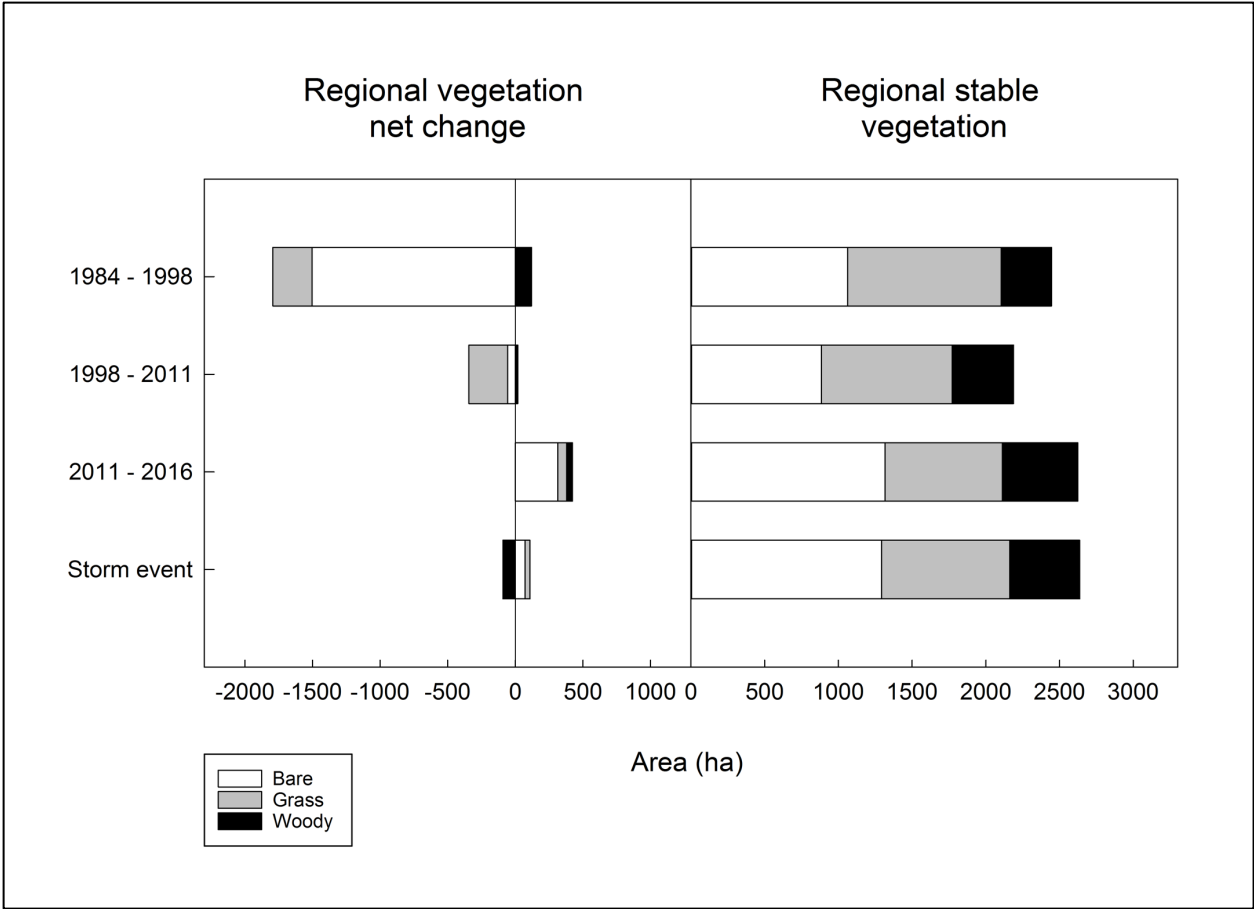
Figure 8: Regional net change and stable area by land cover type and within each period.
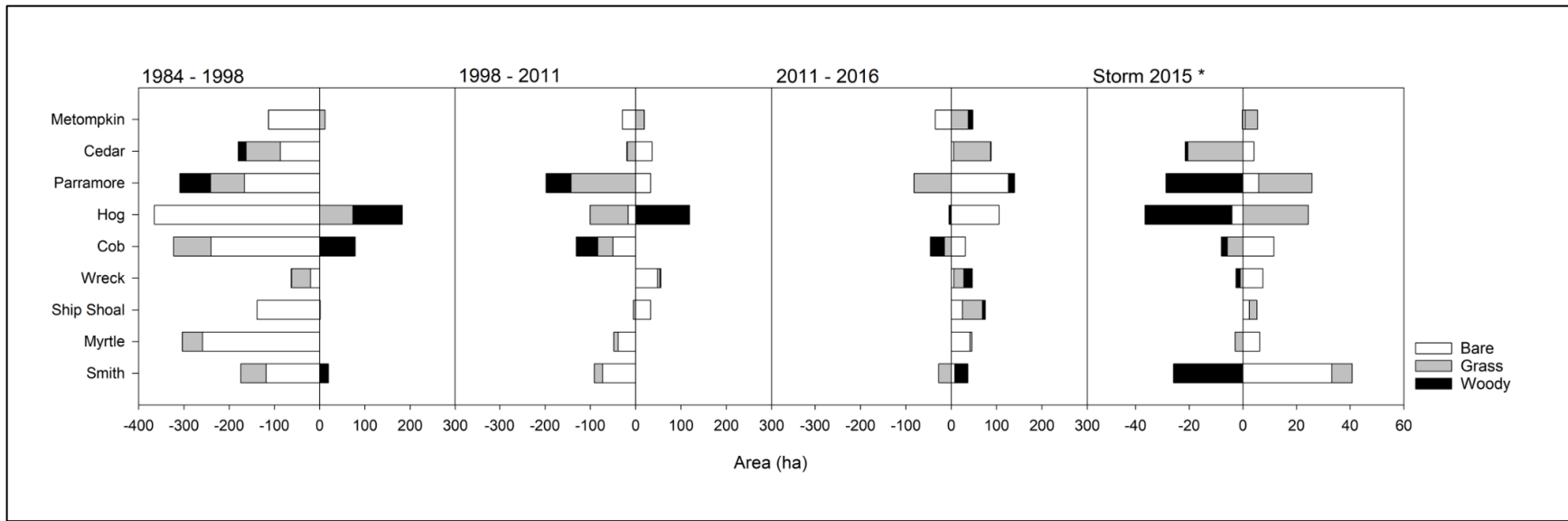
*Figure 9: Island net change by land cover type and within each period. The period marked with * uses a different x-axis range than the other periods.*
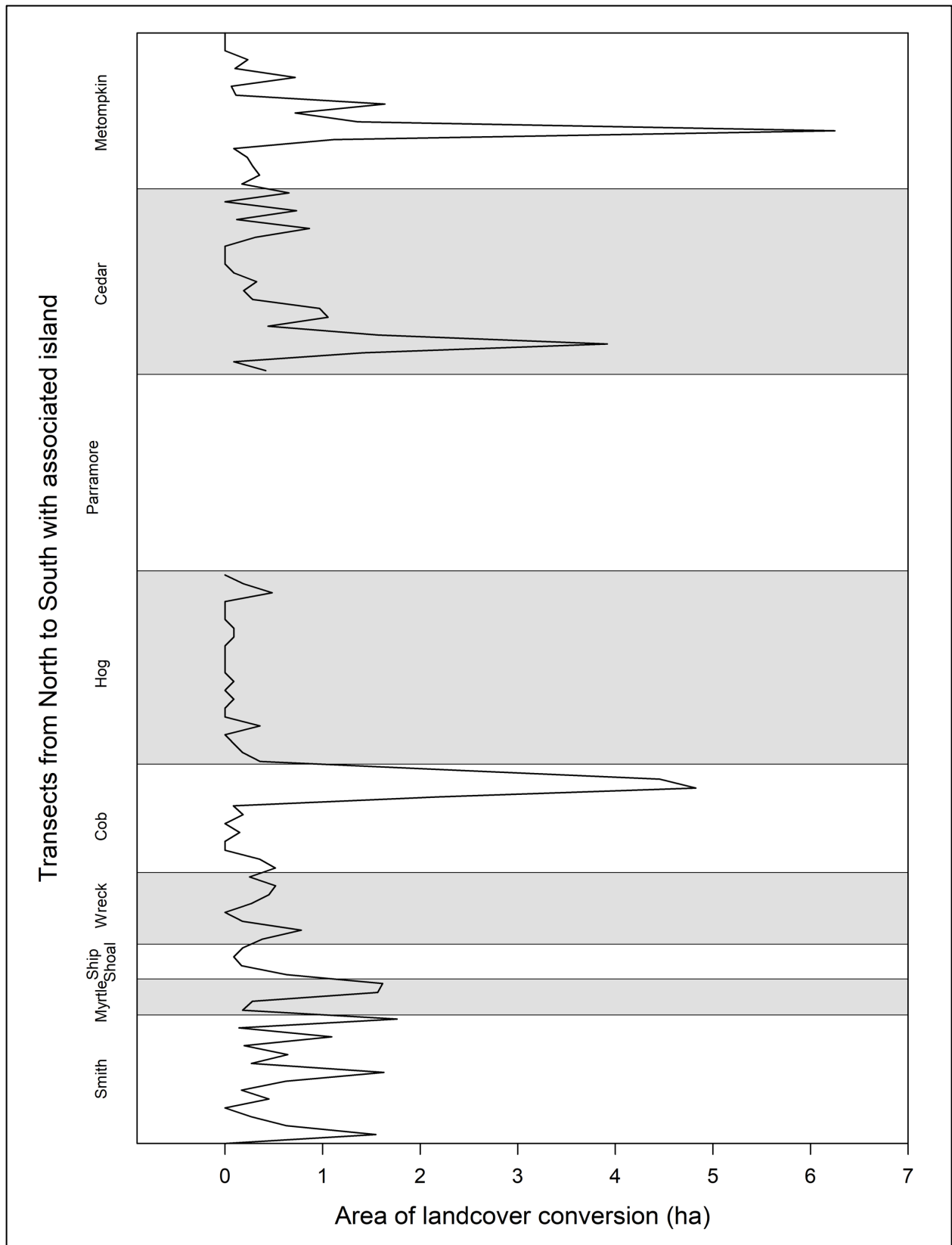
Figure 10: Marsh to upland conversion for each transect across the Virginia barrier islands.

Figure 11: Upland to marsh conversion for each transect across the Virginia barrier islands.

Figure 12: Elevation along the island transects across the Virginia barrier islands.
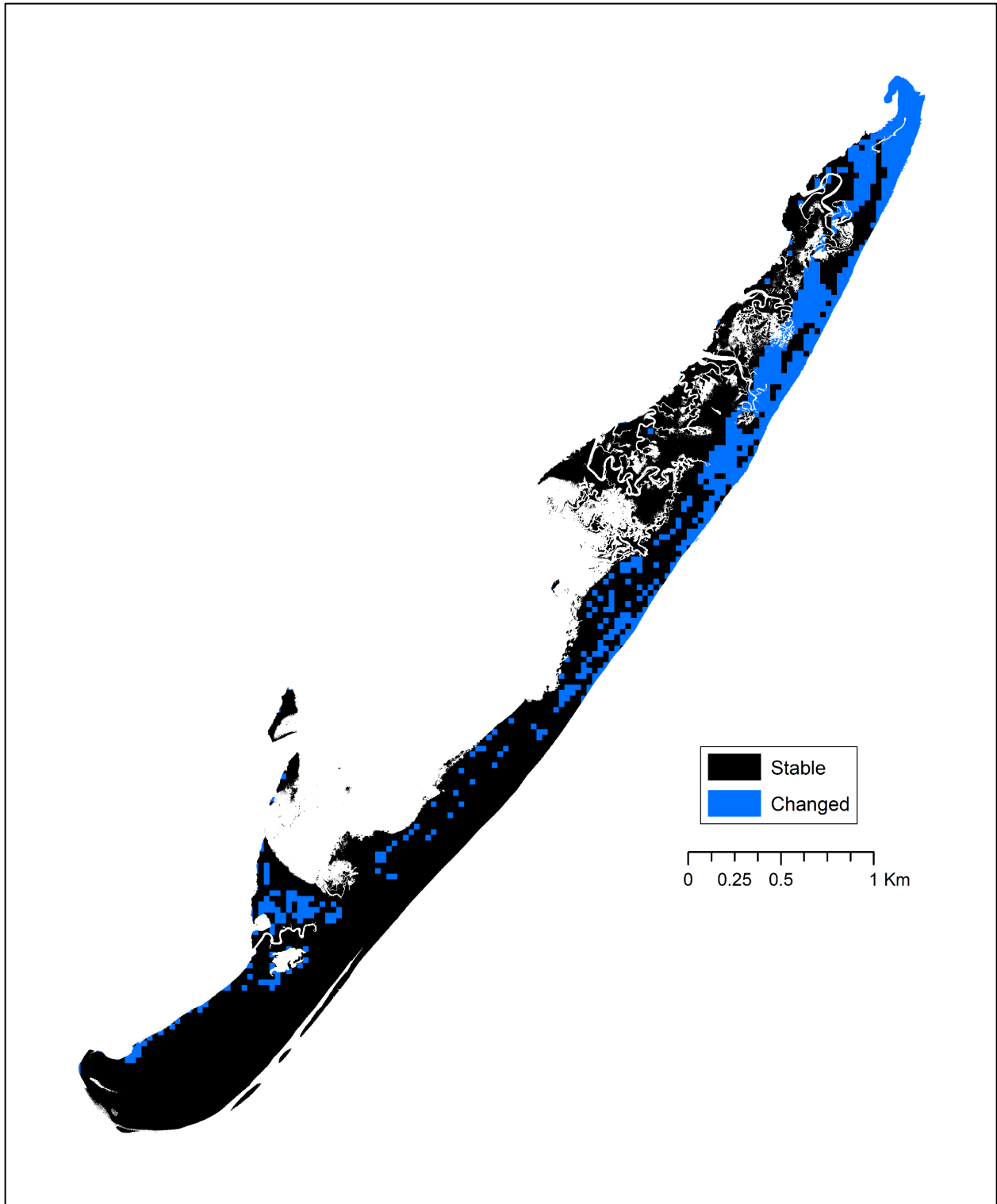
Figure 13: Cobb Island, Virginia vegetation changes post focal storm.

Tables

Table 1: Correlation matrix of elevation and upland cover change for the 2015 storm. Correlation coefficients marked with * is significant at p < 0.05 , with ** is significant at p < 0.01, with *** is significant at p < 0.001, and bold signifies exceeding a 0.5 and -0.5 threshold.

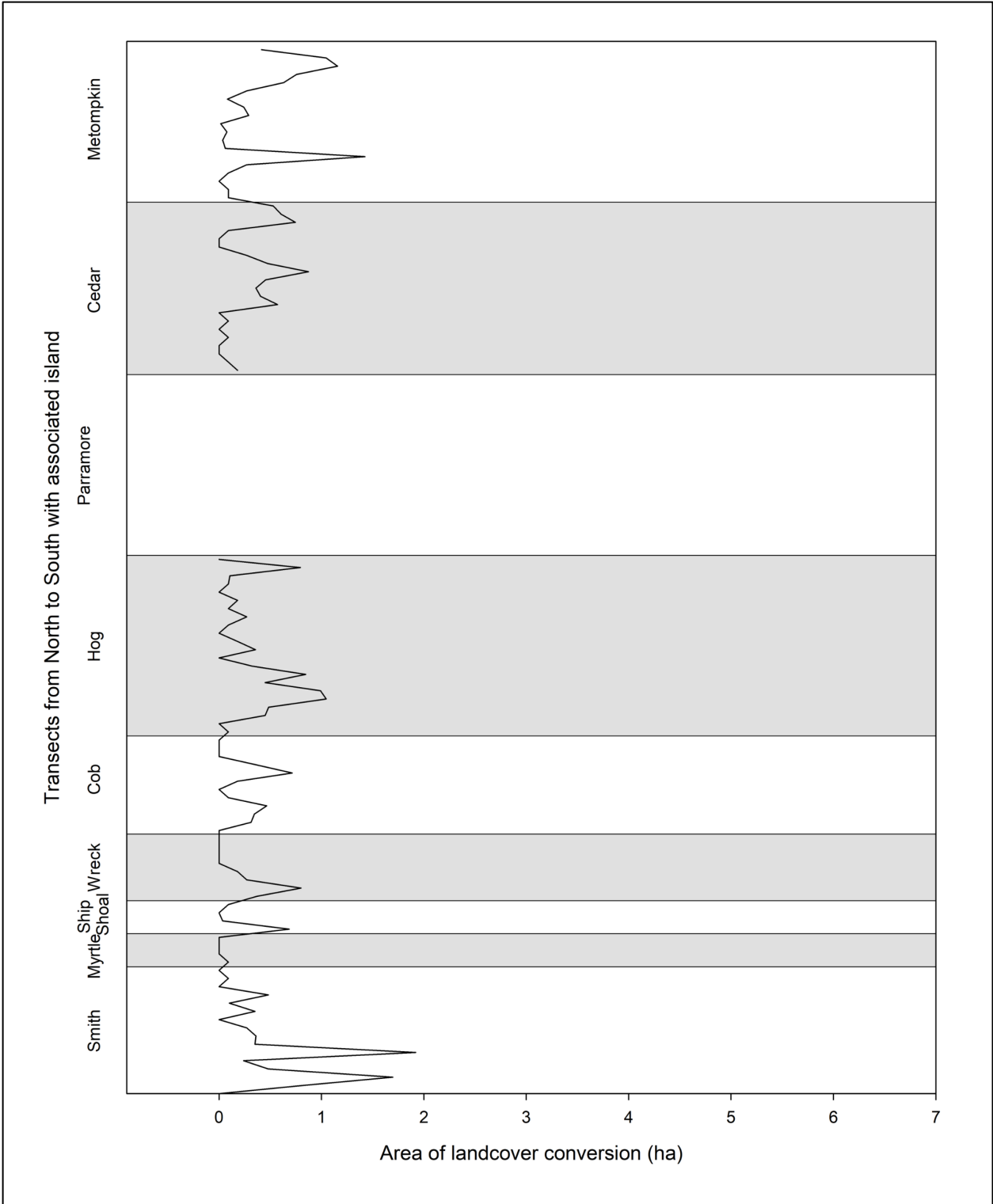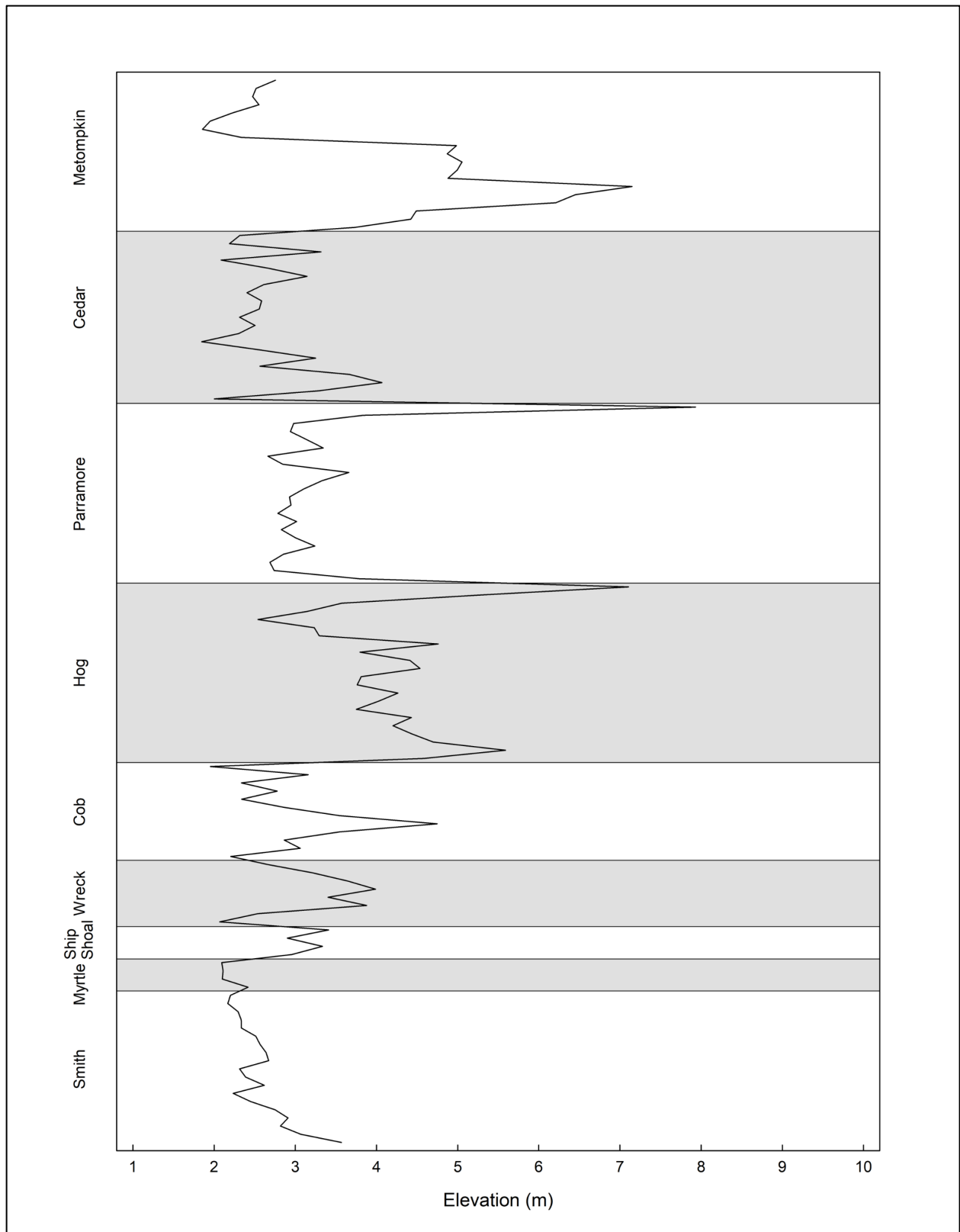|	Maximum bare elevation	Marsh to Upland	Upland to Marsh	Bare, stable	Grass, stable	Woody, stable	Pre Bare	Pre Grass	Pre Woody	Pre Bare (%)	Pre Grass (%)	Pre Woody (%)
Maximum bare elevation	1											
Marsh to Upland	-0.04	1										
Upland to Marsh	-0.04	-0.17	1									
Bare, stable	-0.01	0.17	-0.04	1								
Grass, stable	0.10	-0.25	-0.05	-0.32	1							
Woody, stable	0.41 *	-0.23	-0.26	0.01	0.32	1						
Pre Bare	0.14	0.19	0.00	**1.00 *****	-0.33	-0.03	1					
Pre Grass	0.25	-0.20	0.02	-0.32	**0.99 *****	0.30	-0.31	1				
Pre Woody	0.38 *	-0.22	-0.03	-0.24	**0.57 ****	**1.00 *****	-0.26	**0.60 ****	1			
Pre Bare (%)	-0.34	0.24	-0.04	**0.53 ****	**-0.75 *****	**-0.55 ****	**0.54 ****	**-0.81 *****	**-0.67 *****	1		
Pre Grass (%)	0.21	-0.14	0.08	**-0.48 ****	**0.71 *****	-0.34	**-0.47 ****	**0.80 *****	0.28	**-0.86 *****	1	
Pre Woody (%)	0.36 *	-0.27	-0.01	**-0.37 ***	**0.41 ***	**0.78 *****	**-0.39 ***	**0.47 ****	**0.88 *****	**-0.74 *****	0.29	1

Literature cited

American Meteorological Society. (2012). Storm duration. Glossary of Meteorology. [Available online at http://glossary.ametsoc.org/wiki/climatology.]

Aosier, B., Kaneko, M., & Takada, M. (2007, July). Evaluation of the forest damage by typhoon using remote sensing technique. In 2007 IEEE International Geoscience and Remote Sensing Symposium (pp. 3022-3026). IEEE.

Ayala-Silva, T., & Twumasi, Y. A. (2004). Hurricane Georges and vegetation change in Puerto Rico using AVHRR satellite data. International Journal of Remote Sensing, 25(9), 1629-1640.

Bazzichetto, M., Malavasi, M., Acosta, A. T. R., & Carranza, M. L. (2016). How does dune morphology shape coastal EC habitats occurrence? A remote sensing approach using airborne LiDAR on the Mediterranean coast. Ecological indicators, 71, 618-626.

Brantley ST, Young DR (2007) Leaf-area index and light attenuation in rapidly expanding shrub thickets. Ecology 88:524–530

Brantley ST, Young DR (2009) Contribution of sunflecks is minimal in expanding shrub thickets compared to tem- perate forest. Ecology 90:1021–1029

Brantley, S. T., & Young, D. R. (2010). Linking light attenuation, sunflecks, and canopy architecture in mesic shrub thickets. Plant Ecology, 206(2), 225-236.

Bukata, R. P., Jerome, J. H., Kondratyev, A. S., & Pozdnyakov, D. V. (2018). Optical properties and remote sensing of inland and coastal waters. CRC press.

Carter, G. A., Otvos, E. G., Anderson, C. P., Funderburk, W. R., & Lucas, K. L. (2018). Catastrophic storm impact and gradual recovery on the Mississippi-Alabama barrier islands, 2005–2010: Changes in vegetated and total land area, and relationships of post-storm ecological communities with surface elevation. Geomorphology, 321, 72-86.

Christopoulou, A., Mallinis, G., Vassilakis, E., Farangitakis, G. P., Fyllas, N. M., Kokkoris, G. D., & Arianoutsou, M. (2019). Assessing the impact of different landscape features on post-fire forest recovery with multitemporal remote sensing data: the case of Mount Taygetos (southern Greece). International Journal of Wildland Fire, 28(7), 521-532.

Collins, B. S., & Quinn, J. A. (1982). Displacement of Andropogon scoparius on the New Jersey Piedmont by the successional shrub Myrica pensylvanica. American Journal of Botany, 69(5), 680-689.

Cote, M. R. (2007). Predecessor rain events in advance of tropical cyclones. MS thesis, Department of Atmospheric and Environmental Sciences, University at Albany, State University of New York.

Danilo, C., & Melgani, F. (2019). High-Coverage Satellite-Based Coastal Bathymetrythrough a Fusion of Physical and Learning Methods. Remote Sensing, 11(4), 376.

Davis, R. E., & Dolan, R. (1993). Nor'easters. American Scientist, 81(5), 428-439.

Deaton, C. D., Hein, C. J., & Kirwan, M. L. (2017). Barrier island migration dominates ecogeomorphic feedbacks and drives salt marsh loss along the Virginia Atlantic Coast, USA. Geology, 45(2), 123-126.

Doing, H. (1985). Coastal fore-dune zonation and succession in various parts of the world. In Ecology of coastal vegetation (pp. 65-75). Springer, Dordrecht.

Dolan, R., & Davis, R. E. (1992). An intensity scale for Atlantic coast northeast storms. Journal of Coastal Research, 840-853.

Dolan, R., & Davis, R. E. (1994). Coastal storm hazards. Journal of Coastal Research, 103-114.

ESRI. (2016). ArcGIS Desktop: Release 10.4.1. Redlands, CA: Environmental Systems Research Institute.

Feagin, R. A., Figlus, J., Zinnert, J. C., Sigren, J., Martínez, M. L., Silva, R., … & Carter, G. (2015). Going with the flow or against the grain? The promise of vegetation for protecting beaches, dunes, and barrier islands from erosion. Frontiers in Ecology and the Environment, 13(4), 203-210.

Galarneau Jr, T. J., Bosart, L. F., & Schumacher, R. S. (2010). Predecessor rain events ahead of tropical cyclones. Monthly Weather Review, 138(8), 3272-3297.

Gilbert, M. E., & Ripley, B. S. (2010). Resolving the differences in plant burial responses. Austral Ecology, 35(1), 53-59.

Gornish, E. S., & Miller, T. E. (2010). Effects of storm frequency on dune vegetation. Global Change Biology, 16(10), 2668-2675.

Grinsted, A., Moore, J. C., & Jevrejeva, S. (2013). Projected Atlantic hurricane surge threat from rising temperatures. Proceedings of the National Academy of Sciences, 110(14), 5369-5373.

Hayden, B. P., Dueser, R. D., Callahan, J. T., & Shugart, H. H. (1991). Long-term research at the Virginia Coast Reserve. BioScience, 41(5), 310-318.

Hayden, B. P., Santos, M. C., Shao, G., & Kochel, R. C. (1995). Geomorphological controls on coastal vegetation at the Virginia Coast Reserve. In Biogeomorphology, Terrestrial and Freshwater Systems (pp. 283-300).

Hermosilla, T., Wulder, M. A., White, J. C., Coops, N. C., Pickell, P. D., & Bolton, D. K. (2019). Impact of time on interpretations of forest fragmentation: Three-decades of fragmentation dynamics over Canada. Remote sensing of environment, 222, 65-77.

Houser, C. (2013). Alongshore variation in the morphology of coastal dunes: Implications for storm response. Geomorphology, 199, 48-61.

Houser, C., Wernette, P., & Weymer, B. A. (2018). Scale-dependent behavior of the foredune: Implications for barrier island response to storms and sea-level rise. Geomorphology, 303, 362-374.

Hsu, L. C., & Stallins, J. A. (2020). Multiple Representations of Topographic Pattern and Geographic Context Determine Barrier Dune Resistance, Resilience, and the Overlap of Coastal Biogeomorphic Models. Annals of the American Association of Geographers, 110(3), 640-660.

Huang, H., Zinnert, J. C., Wood, L. K., Young, D., ' D'Odorico, P. (2019, August). Climate warming and microclimate feedbacks drive the expansion of woody species Morella cerifera L. into grasslands in temperate barrier islands. In 2019 ESA Annual Meeting (August—1--16). ESA.

Knapp, A. K., Briggs, J. M., Collins, S. L., Archer, S. R., BRET-HARTE, M. S., Ewers, B. E., ... & Cleary, M. B. (2008). Shrub encroachment in North American grasslands: shifts in growth form dominance rapidly alters control of ecosystem carbon inputs. Global Change Biology, 14(3), 615-623.

Knutson, T. R., McBride, J. L., Chan, J., Emanuel, K., Holland, G., Landsea, C., ... & Sugi, M. (2010). Tropical cyclones and climate change. Nature geoscience, 3(3), 157-163.

Leatherman, S. P. (1982). Barrier island handbook. Coastal Publications.

Leatherman, S. P. (1983). Barrier dynamics and landward migration with Holocene sea-level rise. Nature, 301(5899), 415.

Lee, M. F., Lin, T. C., Vadeboncoeur, M. A., & Hwong, J. L. (2008). Remote sensing assessment of forest damage in relation to the 1996 strong typhoon Herb at Lienhuachi Experimental Forest, Taiwan. Forest ecology and management, 255(8-9), 3297-3306.

Lee, E. Y., & Park, K. (2019). Change in the Recent Warming Trend of Sea Surface Temperature in the East Sea (Sea of Japan) over Decades (1982–2018). Remote Sensing, 11(22), 2613.

Long, J. W., de Bakker, A. T., & Plant, N. G. (2014). Scaling coastal dune elevation changes across storm-impact regimes. Geophysical Research Letters, 41(8), 2899-2906.

Macleod, R. D., & Congalton, R. G. (1998). A quantitative comparison of change-detection algorithms for monitoring eelgrass from remotely sensed data. Photogrammetric engineering and remote sensing, 64(3), 207-216.

Marciano, C. G., & Lackmann, G. M. (2017). The South Carolina Flood of October 2015: Moisture Transport Analysis and the Role of Hurricane Joaquin. Journal of Hydrometeorology, 18(11), 2973-2990.

McBride, R. A., Byrnes, M. R., & Hiland, M. W. (1995). Geomorphic response-type model for barrier coastlines: a regional perspective. Marine Geology, 126(1-4), 143-159.

McCaffrey, C. A., & Dueser, R. D. (1990). Preliminary vascular flora for the Virginia barrier islands. Virginia Journal of Science, 41(4A), 259-281.

Miller, T. E., Gornish, E. S., & Buckley, H. L. (2010). Climate and coastal dune vegetation: disturbance, recovery, and succession. Plant ecology, 206(1), 97.

Morton, R. A., Paine, J. G., & Gibeaut, J. C. (1994). Stages and durations of post-storm beach recovery, southeastern Texas coast, USA. Journal of Coastal Research, 884-908.

Nettleton, B. P. (2018). The role of vegetation-topographic interactions in a barrier island system: Island migration in a changing climate (Unpublished master's thesis). Virginia Commonwealth University.

Otvos, E. G. (2012). Coastal barriers—Nomenclature, processes, and classification issues. Geomorphology, 139, 39-52.

Ozesmi, S. L., & Bauer, M. E. (2002). Satellite remote sensing of wetlands. Wetlands ecology and management, 10(5), 381-402.

Ramsey III, E. W., Chappell, D. K., & Baldwin, D. G. (1997). AVHRR lmagery Used to Identify Hurricane Damage in a Forested Wetland of Louisiana. Photogrammetric Engineering & Remote Sensing, 63(3), 293-297.

Ramsey Ill, E. W. R., Chappell, D. K., Jacobs, D. M., Sapkota, S. K., & Baldwin, D. G. (1998). Resource management of forested wetlands: Hurricane impact and recovery mapped by combining Landsat TM and NOAA AVHRR data. Photogrammetric Engineering & Remote Sensing, 64(7), 733-738.

Ramsey III, E. W., Hodgson, M. E., Sapkota, S. K., & Nelson, G. A. (2001). Forest impact estimated with NOAA AVHRR and Landsat TM data related to an empirical hurricane wind-field distribution. Remote Sensing of Environment, 77(3), 279-292.

Rouse Jr, J., Haas, R. H., Schell, J. A., & Deering, D. W. (1974). Monitoring vegetation systems in the Great Plains with ERTS.

Sallenger Jr, A. H. (2000). Storm impact scale for barrier islands. Journal of Coastal Research, 890-895.

Sánchez-Azofeifa, G. A., Harriss, R. C., & Skole, D. L. (2001). Deforestation in Costa Rica: a quantitative analysis using remote sensing imagery 1. Biotropica, 33(3), 378-384.

Shalaby, A., & Tateishi, R. (2007). Remote sensing and GIS for mapping and monitoring land cover and land-use changes in the Northwestern coastal zone of Egypt. Applied Geography, 27(1), 28-41.

Silva, R., Martínez, M. L., Odériz, I., Mendoza, E., & Feagin, R. A. (2016). Response of vegetated dune–beach systems to storm conditions. Coastal Engineering, 109, 53-62.

Snyder, R. A., & Boss, C. L. (2002). Recovery and stability in barrier island plant communities. Journal of Coastal Research, 530-536.

Spalding, M. D., Ruffo, S., Lacambra, C., Meliane, I., Hale, L. Z., Shepard, C. C., & Beck, M. W. (2014). The role of ecosystems in coastal protection: adapting to climate change and coastal hazards. Ocean & Coastal Management, 90, 50-57.

Stallins, J. A., & Corenblit, D. (2018). Interdependence of geomorphic and ecologic resilience properties in a geographic context. Geomorphology, 305, 76-93.

Stallins, J. A. (2005). Stability domains in barrier island dune systems. Ecological Complexity, 2(4), 410-430.

Stutz, M. L., & Pilkey, O. H. (2011). Open-ocean barrier islands: global influence of climatic, oceanographic, and depositional settings. Journal of Coastal Research, 27(2), 207-222.

Temmerman, S., Meire, P., Bouma, T. J., Herman, P. M., Ysebaert, T., & De Vriend, H. J. (2013). Ecosystem-based coastal defence in the face of global change. Nature, 504(7478), 79.

Thornton, E., Dalrymple, T., Drake, T., Elgar, S., Gallagher, E., Guza, B., ... & Ozkan-Haller, T. (2000). State of nearshore processes research: II.

U.S. Army Corps of Engineers (2013). Coastal Risk Reduction and Resilience. Technical Report ERDC/CHL TR-08-9.

Valderrama-Landeros, L., & Flores-de-Santiago, F. (2019). Assessing coastal erosion and accretion trends along two contrasting subtropical rivers based on remote sensing data. Ocean & Coastal Management, 169, 58-67.

Vinent, O. D., & Moore, L. J. (2015). Barrier island bistability induced by biophysical interactions. Nature Climate Change, 5(2), 158-162.

Wang, W., Qu, J. J., Hao, X., Liu, Y., & Stanturf, J. A. (2010). Post-hurricane forest damage assessment using satellite remote sensing. Agricultural and Forest Meteorology, 150(1), 122-132.

Wijnholds, A. E., & Young, D. R. (2000). Interdependence of Myrica cerifera seedlings and the nodule forming actinomycete, Frankia, in a coastal environment. Journal of Coastal Research, 139-144.

Young, D. R., Sande, E., & Peters, G. A. (1992). Spatial relationships of Frankia and Myrica cerifera on a Virginia, USA barrier island. Symbiosis.

Young, D. R., Erickson, D. L., & Semones, S. W. (1994). Salinity and the small-scale distribution of three barrier island shrubs. Canadian Journal of Botany, 72(9), 1365-1372.

Young, D. R., Shao, G., & Porter, J. H. (1995a). Spatial and temporal growth dynamics of barrier island shrub thickets. American Journal of Botany, 82(5), 638-645.

Young, D. R., Shao, G., & Brinson, M. M. (1995b). The impact of the October 1991 northeaster storm on barrier island shrub thickets (Myrica cerifera). Journal of Coastal Research, 1322-1328.

Young, D. R., Porter, J. H., Bachmann, C. M., Shao, G., Fusina, R. A., Bowles, J. H., ... & Donato, T. F. (2007). Cross-scale patterns in shrub thicket dynamics in the Virginia barrier complex. Ecosystems, 10(5), 854-863.

Zinnert, J. C., Shiflett, S. A., Vick, J. K., & Young, D. R. (2011). Woody vegetative cover dynamics in response to recent climate change on an Atlantic coast barrier island: a remote sensing approach. Geocarto International, 26(8), 595-612.

Zinnert J.C., Shiflett S.A., Via S., Bissett S., Dows B., Manley P., Young D.R. (2016). Spatial–temporal dynamics in barrier island upland vegetation: the overlooked coastal landscape. Ecosystems, 19(4), 685–697.

Zinnert J.C., Stallins J.A., Brantley S.T., Young D.R. (2017). Crossing scales: the complexity of barrier-island processes for predicting future change. Bioscience, 67(1), 39-52.

Zinnert, J. C., Via, S. M., Nettleton, B. P., Tuley, P. A., Moore, L., & Stallins, J. A. (2019). Connectivity in coastal systems: barrier island vegetation influences upland migration in a changing climate.

Vita

Philip Austin Tuley was born on September 5th, 1991, in Richmond, VA. He graduated from Clover Hill High School, Chesterfield County, Virginia in 2010. After career indecisiveness, he attended community college and received his Associate of Science in General Studies with a specialization in Science form John Tyler Community College, Midlothian, VA in 2016. Philip then transferred to Virginia Commonwealth University, Richmond, VA, where he began working as a technician in the Coastal Plant Ecology Lab and fell in love with dynamic coastal systems and GIS. As a technician, Philip's use of these new found loves lead to his first publication. His first undergraduate research focused on comparing time intervals of the relationships between environmental drivers of primary production at the Virginia Commonwealth University Rice Rivers Center. His second undergraduate research was field based and focused on the community disassembly of a relic barrier island maritime forest. After he received his Bachelor of Science in Environmental Studies from Virginia Commonwealth University in 2018, Philip joined the Coastal Plant Ecology Lab to acquire a Master's of Science in Biology. Upon graduating, Philip will optimistically seek employment utilizing the skills he obtained at VCU in GIS, data science, and statistics.